AD-A056 723 MASSACHUSETTS INST OF TECH CAMBRIDGE DEPT OF MECHANI--ETC F/G 20/11
CRACK GROWTH BY CONCENTRATED PLASTIC FLOW.(U)
JUN 78 F A MCCLINTOCK

UNCLASSIFIED

DAHC04-72-C-0043

ARO-10152.1-E

NL

1 OF 1
AD
A056 723

END
DATE
FILMED
9-78
DDC

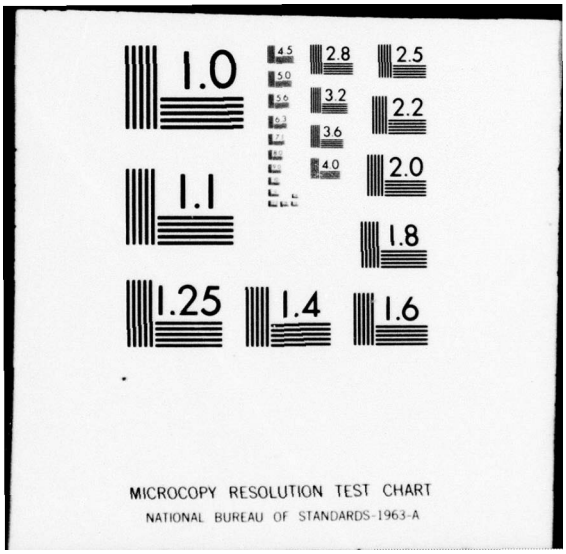
1.0
1.1
1.25
1.4
1.6
1.8
2.0
2.2
2.5
2.8
3.2
3.6
4.0
4.5
5.0
5.6
MICROCOPY RESOLUTION TEST CHART
NATIONAL BUREAU OF STANDARDS-1963-A

CRACK GROWTH BY CONCENTRATED PLASTIC FLOW

Frank A. McClintock

June 28, 1978

U.S. Army Research Office

Contract Number
DAH C04 72 C 0043

220042

Massachusetts Institute of Technology
Department of Mechanical Engineering
Cambridge, Massachusetts

Unclassified

SECURITY CLASSIFICATION OF THIS PAGE (When Data Entered)

REPORT DOCUMENTATION PAGE

READ INSTRUCTIONS BEFORE COMPLETING FORM

1. REPORT NUMBER
2. GOVT ACCESSION NO.
3. RECIPIENT'S CATALOG NUMBER

4. TITLE (and Subtitle)
(6) Crack Growth by Concentrated Plastic Flow

5. TYPE OF REPORT & PERIOD COVERED
(9) Final Report,
1 May 72-31 Oct 75

6. PERFORMING ORG. REPORT NUMBER
--

7. AUTHOR(s)
(19) F. McClintock
Frank A. McClintock

8. CONTRACT OR GRANT NUMBER(s)
(15) DAHC04-72-G-0043

9. PERFORMING ORGANIZATION NAME AND ADDRESS
Mass. Inst. of Techn.
Cambridge, Mass. 02139

10. PROGRAM ELEMENT, PROJECT, TASK AREA & WORK UNIT NUMBERS

(11) 28 Jun 78

11. CONTROLLING OFFICE NAME AND ADDRESS
U. S. Army Research Office
Post Office Box 12211
Research Triangle Park, NC 27709

12. REPORT DATE
June 28, 1978

13. NUMBER OF PAGES
25

14. MONITORING AGENCY NAME & ADDRESS (if different from Controlling Office)
(12) 29 p.

15. SECURITY CLASS. (of this report)
Unclassified

15a. DECLASSIFICATION/DOWNGRADING SCHEDULE

16. DISTRIBUTION STATEMENT (of this Report)

Approved for public release; distribution unlimited.

(18) ARO (19) 10152.1-E

17. DISTRIBUTION STATEMENT (of the abstract entered in Block 20, if different from Report)

18. SUPPLEMENTARY NOTES

The findings in this report are not to be construed as an official Department of the Army position, unless so designated by other authorized documents.

19. KEY WORDS (Continue on reverse side if necessary and identify by block number)

Steel		
Ductility	Plasticity	Fracture Mechanisms
Fracture	Boundary integral method	Notches
Crack growth	Hole growth	Critical stress intensity factor
J-Integral	Fracture transition temperature	Plastic zone size
	5Al6 J_c	Aluminum alloys

20. ABSTRACT (Continue on reverse side if necessary and identify by block number)

A criterion that test specimens be large enough for valid fracture prediction from J_{Ic} tests appears to be that the stress at the half-ligament dimension, calculated from J_{Ic} and the Hutchinson-Rice-Rosengren singularity, be no more than 1.05 to 1.1 times the yield strength. For smaller specimens, the J-integral varied linearly with ligament size and was surprisingly similar for single and double grooved specimens. On the other hand, fully plastic triaxiality was shown to be very important in welded plates of A-36 steel, → next page

DD FORM 1 JAN 73 1473 EDITION OF 1 NOV 65 IS OBSOLETE

Unclassified

SECURITY CLASSIFICATION OF THIS PAGE (When Data Entered)

220 022

in which the transition temperature for brittle crack propagation was raised 40 K above the Charpy value by the triaxiality due to simulated cracks on both sides of the plate. This may also be of interest in fragmentation.

When the J-integral and HRR fields were no longer valid, more crack tip opening in terms of dimple diameter, more sliding-off, and less delamination occurred in the single grooved specimens than in the double grooved ones. The dominant mechanism of crack growth seems to be interactions of holes with the crack tip one at a time.

The crack toughness of a variety of steel and aluminum alloys seemed to be more closely correlated with the yield strain Y/E than with any other microstructural or metallurgical features except cleavage fracture. This fact, along with a review of fracture mechanisms, indicates that the primary possibilities for improvement in fracture resistance are a) for initiation, increasing the adherence between the matrix and second phase particles, and b) for propagation, second phase particles oriented to promote crack meandering and branching.

The difficulty with analysis in the elastic-plastic to fully plastic regimes suggests that more emphasis should be put on realistic tests, such as ones involving plane strain ductility and cracked plates simulating various weld defects.

The boundary integral method using dislocations in internal elements for numerical calculations of plasticity appears to be useful primarily for small plastic zones around cracks in large bodies. Instability of the method eventually developed with non-hardening plasticity. For rate-dependent plasticity (creep), the instability could be suppressed by using a pattern of varying time increments.

Crack Growth by Concentrated Plastic Flow

Table of Contents

1. Introduction

There is a broad need for understanding the fracture of structural alloys at stress levels approaching general yield. Many structures, paticularly in military and transportation fields, are subjected to such loads in service. Under repeated loads, giving low cycle fatigue, one may need to predict the direction of crack growth as well as the rate. In some cases, fracture is intended, as in metal-working operations or in fragmentation. In other cases, one would like to predict failure in large, elastic structures from small, nearly plastic test specimens. Finally, one would like to be able to tell metallurgists how changes in alloys might improve ductility against crack initiation, or toughness against crack propagation. This report summarizes some work directed toward such ends.

We first consider the different mechanisms of fracture in typical structural alloys under various notch configurations. Ideally, from such information, fracture behavior could be derived by mechanics. Currently, service behavior must be predicted from test specimens, so we look at the range of validity of the J integral. We correlate different fracture mechanisms with the different stress states that are found when the criterion is not met.

For crack growth by hole coalescence we present an approximate analysis. For the cleavage fracture mode we show by some experiments on cracks and notches at defective welds in steel that present test configurations may not be conservative, indicating the need for a wider range of test specimen configurations.

Finally, we report on the prospects for development of computer programs useful for further numerical work either for structures to determine the stress and strain in the neighborhood of the fracture process zone, or for microstructures to estimate crack formation and growth. A condition for stable explicit integration of creep equations is suggested.

2. Fracture Mechanisms

Fracture initiation in metals under monotonic load has been investigated over a number of years. The fracture site in the center of a necked specimen was observed by Ludwik (1926) and an approximate stress analysis carried out by Bridgman (1952). Cleavage fracture in steel at low temperatures was recognized early. The mechanism of hole growth from inclusions was identified by Tipper (1949) although it was the electron micrographs of Plateau, Henry, and Crussard (1956) that brought a wide understanding. The micromechanics of growth of non-interacting holes was developed by McClintock (1968), Rice and Tracey (1969), and Tracey (1971), but tends to over-estimate the ductility. Preliminary estimates of the limitation of ductility by localized flow between holes were made by Nagpal, et al. (1973), but better analysis is needed for the beginning of concentrated flow by hole interaction in metals with a history of slight strain-hardening.

For crack growth, several mechanisms have been reported.

a) A sharp crack growing either by continuous blunting (Rice and Johnson, 1970), (Joyce, 1968), by alternating sliding off as a sharp V (Joyce, 1968), (Elliott and Stuart, 1968), (Hayden and Floreen, (1969),

or by several such wedges.

b) A crack growing by successive interactions with a single hole, as suggested by Cipolla (1973).

c) Individual voids so numerous as to constitute a continuum.

d) The localization of flow in a dilating continuum (Berg, 1970), followed by the joining up of the individual voids within the band (Nagpal, et al., 1973) giving, in effect, traction-displacement boundary conditions on the surrounding material.

Means of handling each of these crack formation and growth mechanisms must be included in any general numerical program by allowing for concentrated flow elements, arrays of holes, dilational plasticity, general compliant and interactive boundary conditions. Experiments are still required, however, to decide which mechanisms are most important and therefore which should be analyzed first.

3. Valid J-Integral Specimens for Crack Instability

(Summary of Joyce and McClintock (1976), with added notes on fractography).

Tests on a variety of alloys, with the specimen configuration of Fig. 3.1, led to a criterion for valid J-correlation of crack instability. Assume an Ilyushin stress strain curve with exponent n, stress at unit strain $\bar{\sigma}_1$, fitted to the total stress-strain curve at the yield point σ_Y and the fracture point:

$$\bar{\sigma} = \bar{\sigma}_1 (\bar{\varepsilon})^n . \qquad (3.1)$$

The correlation is based on the idea that a certain stress ratio is

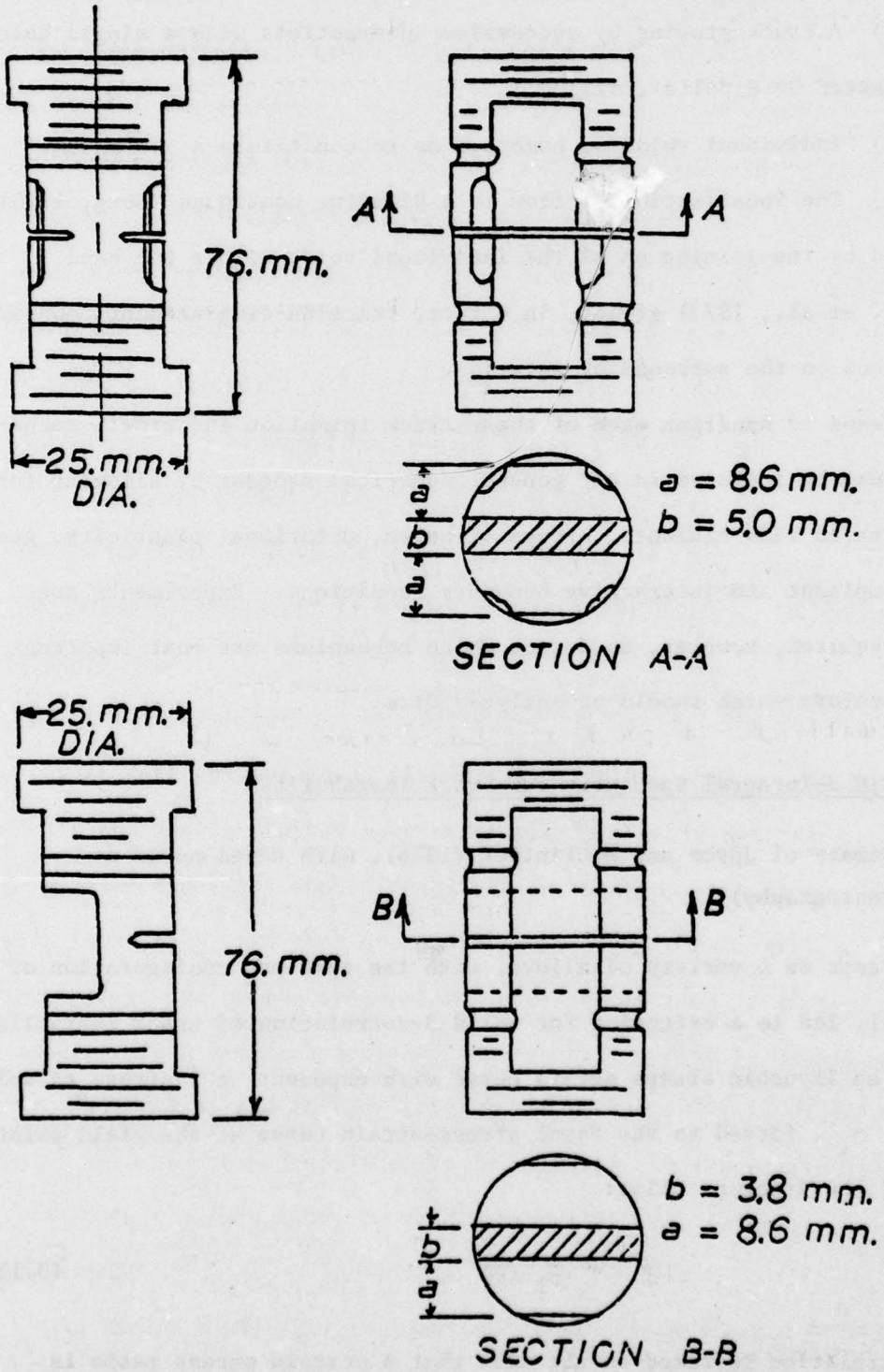

Fig. 3.1, Double and Single Grooved Specimen Geometries

required to develop the Hutchinson-Rice-Rosengren (HRR) non-linear stres field, within a region small compared to the specimen ligament dimension b but large compared to the crack tip opening displacement, discussed further in Section 5,

$$\text{CTOD} = 2\, J/I_n \bar{\sigma}_1 \,. \tag{3.2}$$

The required radius r_{HRR} for a valid HRR singularity is then given in terms of a stress ratio c by

$$b/2 > r_{HRR} = \frac{J_{I_c}}{I_n \bar{\sigma}_1} \left(\frac{\bar{\sigma}_1}{c\sigma_y} \right)^{(n+1)/n} \,. \tag{3.3}$$

With a value of c = 1.1, the criterion successfully distinguished between specimens with valid and invalid J-correlations, as judged by the same J_{Ic} and the same fractographic features for both the single and the double grooved specimens. Similar success was found for a range of steels, except that for the higher strength steel, the factor c must be taken to be 1.05. While the difference appears small, the low exponent n makes this difference in constants c significant. The semi-empirical nature of this correlation, and the fact that it does not take into account differing states of stress and strain in the corresponding non-hardening solutions, mean that further experiments and also numerical calculations of the stress and strain fields for strain hardening exponents of the order of 0.1 would be very desirable.

4. Fractographic Observations

Specimens of 2024-T4 and 7075-T651 aluminum alloys with ligaments as small as 1.91 mm gave apparently valid J_{Ic} values of 0.026 and

0.036 MJ/m^2. Values of K_{Ic} calculated from these J_{Ic} values were found to be larger by 30 to 50% than handbook K_{Ic} values for these materials. This difference might have resulted from the different forming processes of the specimens. Any difference due to crack initiation occurring before maximum load in these materials is likely to be less than 20%, judging from fatigued-loaded-fatigued specimens. The initial fracture topography of the single and double grooved specimens was identical. The crack tip blunting and the average dimple diameter are on the order of the CTOD, in agreement with Rice (1973). Fracture was by void growth and coalescence and occurred before the limit load was reached.

The fatigued-loaded-fatigued specimens of 2024-T4, 7075-T651, and 6061-T6 showed that at most one hole was opening in front of the crack tip. No bands of localized flow were observed which had grown in advance of the crack tip.

In 6061-T6 aluminum and cold-finished 1117 steel, for which valid J_{Ic} results were not obtained, the initial fracture surface topographies for single and double grooved specimens were noticeably different. The double grooved specimens showed delamination, a sharp step at the fatigue-fracture transition, and then an abrupt transition to hole growth fracture. The step height was on the order of the CTOD, which in turn is equal to approximately five dimple diameters. On the single grooved specimens, no step was observed at the fatigue-fracture transition. Instead, a combination of hole growth and sliding off is observed. A transition to pure hole growth then occurs about 20 dimple diameters from the root of the fatigue crack.

In a hardened high-purity aluminum alloy, valid J tests were not

found. Initial fracture topographies were very similar for single and double grooved specimens. In specimens with cracks normal to the width direction W , growing in the thickness direction T (WT orientation), and also in ones with the RT orientation, fracture occurred by delamination consisting of hole growth in the plane normal to the direction. The average dimple spacing was 0.8 μm and inclusions of approximately 0.15 μm diameter were visible in the center of many of the dimples. The TW specimens do not show a hole growth fracture mechanism, which is a surprise since the fracture occurred in the same plane which delaminated by hole growth in the WT and RT specimens. Instead, the fracture surface consisted of steps with a wavy, featureless appearance.

5. Predicting Crack Toughness from Microstructure

(Excerpts from McClintock, 1977)

Take as a measure of the crack toughness of a material the critical plastic zone size for instability, r_{Yc} given in terms of the critical stress intensity factor K_{Ic} and the yield strength Y for a nonhardening material by Levy, et al (1971):

$$r_{Yc} = \frac{1}{2\pi}\left(\frac{K_{Ic}}{Y}\right)^2 \qquad (5.1)$$

Most alloys whose fracture is of concern are so lightly strainhardening ($n \approx 0.1$) that Eq. 5.1 is a good approximation.

It is the critical value of this plastic zone size, r_{Yc}, not K_{Ic} itself, that should be tabulated as a material property characterizing crack toughness because its dimensions are those of length and are much more easy to visualize than $FL^{-3/2}$. In particular:

1. The designer can directly compare r_{Yc} with the dimensions of his part. If the calculated r_{Yc} is greater than the ligament dimension, the part will carry its fully plastic limit load before fracture (although fracture may still reduce the extension of the part).

2. r_{Yc} gives a rough measure of the maximum allowable half-length of a crack that can withstand working stresses up to a large fraction of the yield strength. Specifically, up to about half the yield strength, the relation for K_I in terms of crack half length c and applied stress at "infinity" σ_∞,

$$K_I = \sigma_\infty \sqrt{\pi c} , \tag{5.2}$$

and Eq. 5.1 combine to give

$$c_c = \frac{1}{\pi}\left(\frac{K_{Ic}}{\sigma_c} \right)^2 = \frac{r_{Yc}}{2} \left(\frac{Y}{\sigma_c} \right)^2 . \tag{5.3}$$

For instance, for a maraging steel with a reasonably tough-sounding value of K_{Ic} = 90 MN/m$^{3/2}$ (83,000 lb/in.$^{3/2}$) and a yield strength of 1806 MN/m^2 (262,000 psi), the critical plastic-zone size is only 0.39 mm. Cracks down to about this size would have to be found and eliminated, unless one adopts fail-safe design or is willing to pay off on failures.

3. The plane strain r_{Yc} can be compared directly to the specimen thickness. The plane-strain assumption is valid if the part is thicker than about 6 times the plane-strain critical plastic-zone radius.

4. If r_{Yc} approaches the ligament dimension, nonlinear elastic fracture mechanics (the J-integral) must be used.

5. For nonhardening materials, the flank-to-flank crack-tip opening displacement can be readily pictures in terms of the plastic-zone radius by

$$\text{CTOD} = 2.7\, r_Y\, Y/E \,. \tag{5.4}$$

5.1 Displacement criterion for crack initiation

Now return to estimating the fracture toughness at initial crack growth, r_{Yi}, from the inclusion half spacing ℓ assuming

$$\text{CTOD}_i = 2\ell \,. \tag{5.5}$$

For a nonhardening material, Eq. 5.4 gives

$$r_{Yi} = 0.37\, (2\ell)\, (Y/E) \,. \tag{5.6}$$

For a hardening material, the near tip stress, strain, and displacement fields can be given in terms of the J-integral, which can be thought of as a scalar, like K_I. These fields hold for a nonlinear, elastic, incompressible stress-strain relation of the form

$$\sigma = \bar{\sigma}_1\, \varepsilon^n \,. \tag{5.7}$$

If Eq. 5.7 represents the total strain, the nonlinear-elastic or deformation theory plasticity gives the same result as the more physical incremental plasticity. It is not valid for crack growth, wherein the ratios of strain increments change as the crack passes by. For most alloys, the exponent n is of the order of 0.05 to 0.25. The constant $\bar{\sigma}_1$ can be thought of as the equivalent stress at unit strain. The nonlinear stress and strain fields also depend on a numerical coefficient I_n that varies slowly with n within 2 percent of (Joyce and McClintock, 1976)

$$I_n = 10.3\, \sqrt{0.13 + n} - 4.8n \,. \tag{5.8}$$

In terms of these quantities and normalized stress, strain, and displacement functions which depend only on angle, the Hutchinson (1968a,b) Rice and Rosengren (1968) (HRR) fields are

$$\frac{\sigma_{ij}(r_1\theta)}{\bar{\sigma}} = \left(\frac{J}{\bar{\sigma}_1 I_n r} \right)^{n/(n+1)} \tilde{\sigma}_{ij}(\theta) \ .$$

$$\varepsilon_{ij}(r,\theta) = \left(\frac{J}{\bar{\sigma}_1 I_n r} \right)^{1/(n+1)} \bar{\varepsilon}_{ij}(\theta) \ . \qquad (5.9)$$

$$\frac{u_i(r,\theta)}{r} = \left(\frac{J}{\bar{\sigma}_i I_n r} \right)^{1/(n+1)} \bar{u}_i(\theta) \ .$$

At the flank of a crack, the normalized displacement function $\tilde{u}_i(180°)$ is unity. The desired flank-to-flank opening, where $r = u$, is then

$$\text{CTOD} = \frac{2J}{I_n \bar{\sigma}_1} \ . \qquad (5.10)$$

Equation 5.10 gives perhaps the most direct physical insight into the meaning of J. Since the deformation theory stress strain relation of Eq. 5.6 is not at all valid for crack growth, the interpretation of J as a strain-energy release rate is not physically very useful, even though it is provided the insight for the original derivation.

When the plastic zone is extending nearly all across the specimen, J must be evaluated numerically for the particular structure and loading. When there is a surrounding linear elastic stress singularity, J can be found from K :

$$J = K_1^2 (1 - \nu^2)/E \ . \qquad (5.11)$$

In terms of the nonhardening plastic-zone radius,

$$J = 2\pi \, r_Y \, Y^2 (1 - \nu^2)/E \ . \qquad (5.12)$$

Finally, we can relate the critical plastic-zone size for crack initiation to the spacing between hole nuclei by combining Eqs. 5.5, 5.10, and 5.12:

$$r_{Yi} = \ell \frac{I_n}{2\pi} \frac{E\bar{\sigma}_1}{Y^2(1 - \nu^2)}, \quad \text{with } \nu = 0.5 \ . \qquad (5.13)$$

For a nonhardening material this reduces to $r_{Y1} = 0.39\ (2\ell)E/Y$, compared to $0.37(2\ell)E/Y$ obtained from Eq. 5.6. For a hardening material with $n = 0.1$, $Y/E = 0.004$, $Y/\sigma_1 = 0.174$, $r_{Yi} = 0.822(2\ell)E/Y$, indicating a rather strong effect of strain hardening.

5.3 Crack Instability

There is not much prospect of a closed form analytical solution for a growing Mode I crack, taking into account geometry changes, the incremental flow rule, strain hardening, residual stresses, and the strained material left behind the growing crack. Perhaps some insight can be obtained from the Mode III solutions (shear parallel to the leading edge of the crack). The most unrealistic feature is that in Mode III the plastic zone extends mostly in front of the crack, so the crack advances into prestrained material, whereas for initial Mode I loading the plastic zone runs off to the side. This discrepancy is likely to be reduced by strain hardening, residual stress, and possible zigzagging of a Mode I crack.

With these caveats, the Mode I analogue of Mode III instability is given in terms of the fracture strain ε_f^P (perhaps including any needed to initiate holes and only the further strain to the point of localization), McClintock (1971):

$$r_{Yc} = 2\ell \exp\left[\sqrt{2\varepsilon_f^P/(Y/E) + 1} - 1\right] . \tag{5.14}$$

5.4 Strain criterion for initiation. The analogue of Eq. 5.14 for initiation is:

$$r_{Yi} = 2\ell \left(\varepsilon_f^P/(Y/E) + 1\right) . \tag{5.15}$$

5.5 Comparison with data. The estimates for initiation by displacement (Eq. 5.13) and strain (Eq. 5.15) and for instability (Eq. 5.14) are given in Table 2.5 for the three aluminum alloys and the 1117 cold-finished steel studied by Joyce (1974). The hole growth ratio was taken roughly from his scanning electron micrographs. The fracture strain was assumed to consist entirely of that required to grow the holes to coalescence. An approximate equation, exact for zero or linear hardening and equi-axial transverse strain and axial shortening of cylindrical holes has been obtained by McClintock (1968). The rate of change of semi-minor axis a of holes spaced $2\ell_a$ apart, subject to applied stress of σ_a^∞ and σ_b^∞ and internal pressure p, in a material with an equivalent flow strength Y undergoing an equivalent strain increment of $\varepsilon^{-\infty}$ is

$$d\ \mathrm{In}(a/\ell_a)/d\varepsilon^{-\infty} = \sinh[(1-n)(\sigma_a^\infty + \sigma_b^\infty + 2p)/(2Y/\sqrt{3})]/(1-n) . \tag{5.16}$$

Note that in the limit as the strain-hardening exponent n approaches 0

the hole growth rate becomes exponential with the applied stress, whereas for linear hardening, $n = 1$, the hole growth rate per unit applied-strain increment varies linearly with the applied stress. Equation 5.16, for the stress ratio $(\sigma_a^\infty + \sigma_b^\infty)(2Y/\sqrt{3})$ of $3/2 + \pi$, expected in front of a crack, was used to obtain the fracture strain needed in Eqs. 5.14 and 5.15 at the observed hole growth ratio.

Table 5.1 Initial and Critical Plastic Zone Radii

						Initiation, f_{Yi}		Instability, f_{Yc}	
						Strain	Displac.	Strain	
Alloy	Y, MN/m^2	E, MN/m^2	n	2ℓ, mm	$\frac{(\ell_a/a)_f}{(\ell_a/a)_{f_i}}$	Eq.5.13 mm	Eq.5.15 mm	Eq.5.14 mm	Observed mm
7065-T6	500	72,000	0.10	0.012	3	1.42	0.064	0.1	1.34
				0.016	4	1.89	0.104	0.189	
2024-T4	390	72,000	0.12	0.012	3	1.82	0.084	0.163	3.39
				0.040	3	6.07	0.281	0.544	
6061-T6	281	72,000	0.09	0.012	6	2.53	0.159	0.689	11.
1117 steel	510	200,000	0.07-0.11	0.004-0.020	5	1.89-6.44	0.332-0.377	2.14-3.13	>25.

For the stronger alloys of Table 1, the displacement-based plastic zone size for initiation, r_{Yi}, is comparable to the critical value, as has been noted by others. The displacement-based criterion fails, however, to predict the very large increases in plastic zone radii in alloys with low yield strain Y/E.

The strain-based criteria show relatively little difference between initiation and instability for the strongest alloys, but much more for the

weaker ones, in line with experience. The theoretical level of r_Y is too low for all the strain criteria. Possible reasons include crack blunting with loss of triaxiality, lack of strain hardening in Eq. 5.14, and advance of the crack into unstrained material. Detailed numerical work appears necessary, in addition to any possible analytical results.

6. A Grooved-Strip Test for Weld Ductility

6.1 Introduction

The question examined here is whether an improved test specimen can provide a better measure than the Charpy V-notch for the practical performance of plates and welded structures. Because it would be desirable for welded structures to become fully plastic before fracture, even in the presence of a crack, and because analytical and numerical methods for determining the ductility of a large plate in terms of the Charpy behavior, or critical stress intensity factor, for example, are not known for the fully plastic case, Marcolini (1975) carried out a test on specimens containing defects as near to full scale as practical.

6.2 Material and welding.

The chemical composition of the A-36 base metal was 0.21% C, 0.69% Mn, 0.04% Si, 0.015% P, and 0.018% S. Properties in 13 mm plate were 279 MN/m^2 (40,400 psi) yield, 439 MN/m^2 (63,600 psi) tensile strength, and 27% elongation in 203 mm (8 in.).

Two manual submerged arc-weld passes were made with a 2 mm (5/64 in.) diameter L-60 electrode/860 flux combination (Lincolnweld R, Classification F62-EL12). Tests required by specifications AWS A5.17-69. ASME SFA 5.17 showed the chemistry and mechanical properties of the deposited

weld metal, according to the test certificate for this flux-electrode combination, to be 0.077% C, 0.88% Mn, 0.22% Si, 0.019% P , and 0.015% S , with a yield of 405 MN/m^2 (58,800 psi), a tensile strength of 484 MN/m^2 (70,200 psi), an elongation in 51 mm of 29%, and Charpy V-notch impact properties of 85 Nm (63 ft lb) at 244 K (-20 F).

For the largest practical test with available equipment, strips of plate 12 mm thick by 76 mm wide were welded. Surface cracks were simulated by machining grooves 2 mm deep for 9.5 mm with a 102 mm dia. cutter, in the face of the strip and parallel to the weld, at various locations base metal, weld metal and heat-affected zone (HAZ). The strips were then subjected to alternating bending in an SF1 fatigue testing machine of ±340 Nm (3000 in.-lb) capacity. Strips of this size could be pulled in a 0.9 MN (200,000 lb) hydraulic testing machine. Adequate ductility is indicated by a significant reduction of area in the minimum section and a hole growth mode of fracture as the crack progresses out of the pre-cracked semi-elliptical zone into the unnotched edges of the strip.

6.3 Results

The principal results are shown in Table 3.1. Charpy tests showed a severe degradation of behavior in the heat-affected zone, where the transition temperature at least was 294 K, as contrasted to 255 to 263 K in the base and weld metals. For the singly grooved strip, the fracture appearance transition temperature for the base metal and the heat affected zone were much more nearly comparable (250-260 K). The transition temperatures as indicated by thinning of either the center section or the unnotched edge section were very nearly the same as the fracture appear-

ance transition temperature. This is likely because all three transitions were concerned with a growing crack. With doubly grooved specimens, however, (which did not contain a fatigue crack extension) the fracture appearance transition temperature after the crack began to run was greater than 299 K. The crack was ductile in traversing the thickness, but changed to cleavage as it spread laterally. Note that a specimen as small as a Charpy specimen would have indicated complete ductility under these circumstances. It would erroneously have indicated safe behavior. In the wider strip the crack apparently became unstable, picked up speed and changed to a cleavage mode, which would be catastrophic in a large structure. Similar doubly-grooved behavior was observed for the base metal.

6.4 Conclusion

Apparently, the increased triaxiality due to two grooves opposite each other, led to a 40 K rise in fracture transition temperatures for A-36 steel. Furthermore, the material does not respond to these grooves (potential defects) in the same way that the Charpy specimen does. The Charpy specimen may be either over- or under-conservative, depending on the conditions. There is, therefore, a need for improved tests that more closely simulate service conditions, until such time as theory and numerical methods can provide quantitative predictions. Similar results would be expected in fragmentation.

Table 6.1 Fracture data for welded, grooved strips of A-36 steel
12.7 x 76 mm, 610 mm long, 254 mm between grips

No.	Total crack depth	Temp.	Load rate $\frac{A_{gr}}{TS}$	Center thinning	Edge thinning	Crack opening angle	Fracture mechanism
	mm	K	s^{-1}	%	%	°	
	Base metal						
Base							
-1	8.7	247	2.91 E-3	1.6	6.1	0	cleavage
-5	6.8	248	0.95 "	3.9	4.4	4	mixed
-6	5.9	250	1.39 "	8.4	18.	15	hole growth
-4	7.7	256	1.54 "	8.7	19.	24	hole growth
-3	8.7	256	0.21 "	8.7	17.	22	hole growth
-2	7.1	265	0.92 "	6.8	5.6	5.4	mixed
-7	4.1	299	1.50 "	1.2	4.4	-	mixed
	(Double groove, 2 mm each side, no fatigue cracking.)						
	Heat-affected zone						
HAZ							
-4	8.0	247	2.62 E-3	0.0	3.5	0	cleavage
-7	6.4	249	0.82 "	0.0	1.7	0	cleavage
-6	6.2	258	0.70 "	9.4	14.1	18	hole growth
-5	6.9	263	0.98 "	8.3	10.2	25	
-2	5.8	275-286	0.1-0.16"	8.4	12.9	19	
-3	3.2	280-286	0.1-0.16"	6.2	6.6	10	
-1	5.9	286-292	0.1-0.16"	9.4	13.1	19	
-9	5.5	299	18.9 "	7.2	10.1	10	
-8	3.7	303	12.2 "	9.8	18.2	17	
-10	4.1	299	1.3	0.0	3.5	-	mixed
	(Double groove, as above)						

7. Numerical Studies

Joyce (1974) developed a numerical method for plastic plane strain analysis based on boundary integral, stress relaxation techniques. The method was extended to creep by Ebisu. The method is based on an elastic boundary integral program implementing the following scheme:

a) Boundary conditions can be of the most general linear type, giving a number of loading parameters P^k as linear functions of the components of traction (force per unit surface area, t^μ) and displacement u^μ of each boundary segment μ.

$$P^k = P_t^{k\mu}\, t^\mu + P_u^{k\mu}\, u^\mu \,. \tag{7.1}$$

(For example, traction boundary conditions are met by setting $P_t^{kk} = 1$, all other terms zero). These general boundary conditions allow treating the fracture mechanisms of Section 2. It would be very desirable to extend the capabilities of finite element programs to include them. (For the boundary integral method, in order to satisfy moment equilibrium, it is necessary to include moments, normally zero, applied to each segment which are, in effect, gradients of the normal traction, t_{ng}. (Shear gradients of traction and gradients of displacement are included for completeness and improved accuracy, although for simplicity they will not be included in the following discussion).

b) With the body modeled as being embedded in an infinite matrix, relative displacements are inserted between the body and the matrix. At either end of any given segment m there is then a pair of edge dislocations, called darts, D^m. The known stress fields of dislocations give

the tractions t^{μ} and displacements u^{μ} on the affected segments μ due to the dislocated segments m. Summing over all segments,

$$t^{\mu} = T^{\mu m} D^{m} , \quad u^{\mu} = U^{\mu m} D^{m} . \tag{7.2}$$

c) Substitution of Eqs. 7.2 into 7.1 gives an equation for the unknown darts in terms of the parameters of the boundary conditions, which can then be solved for the darts:

$$P^{k} = \left(P_{t}^{k\mu} T^{\mu m} + P_{u}^{k\mu} U^{\mu m} \right) D^{m} .$$

d) With the darts known, the stresses at any interior points can be found.

e) Plasticity is modeled by subdividing the interior into elements. Within the elements, strain is modeled by dislocations migrating to the element walls. The resulting dislocation arrays reduce the stresses and modify the boundary tractions and displacements. Their effects are added to Eqs. 7.2 and the process is repeated.

The program was developed to a working state, but it turned out that instabilities developed after long times. These instabilities also appear in explicit integration of rate-dependent plasticity (creep) with the finite element method. Ebisu, in unpublished work supported by the project showed that short time increments re-stabilized the calculations, allowing a few long time intervals before instability reappeared. In rate-independent plasticity, a subsequent one-dimensional analysis indicates that the method is inherently unstable, although the instability shows up slowly enough so that some problems can be solved.

While the boundary integral method developed here requires solving

fewer simultaneous equations than the finite element method, the matrices are fully dense, not sparse, and very large numbers of influence coefficients are required. It appears to be useful primarily for small plastic zones around cracks in large bodies. For instance, it has been successfully applied to the cracks in railroad rails, under complex histories of compression and shear (McClintock, 1977).

8. Conclusions

1. Singly and doubly grooved, plane strain tensile specimens cut from 25 mm D bar stock were used to test the validity of the Hutchinson-Rice-Rosengren (HRR) J-integral correlation. A criterion based on a desired stress ratio in the HRR field indicates valid results if the stress at the half-ligament dimension is no more than 1.05 to 1.1 times the yield strength. For smaller specimens, the J integral varied linearly with ligament size and was surprisingly similar for single and double grooved specimens.

2. In the valid J region for high strength aluminum alloys, crack initiation occurred at a crack tip opening of the order of one hole spacing. Crack growth occurred by successive interaction of one hole at a time with the crack. In specimens of 6061-T6 aluminum and cold finished 1117 steel, with invalid J criteria, single and double grooved specimens failed by different mechanisms. The double grooved specimen showed delamination, a sharp step at the point of fracture initiation, and then an abrupt transition to hole growth. For 6061 T6, the step height was of the order of five hole diameters. Only on the single grooved specimens of these alloys was sliding off observed. The transition to hole growth occurred after 20 hole diameters of CTOD.

3. Plates of a high purity aluminum zinc alloy exhibited very anisotropic fracture behavior, sometimes with a wavy featureless appearance rather than hole growth.

4. A theoretical prediction of the critical plastic zone size from fractographic observations shows that the displacement concept failed to indicate the very large increases in plastic zone in alloys with low Y/E. A criterion based on a critical strain and an analogy with Mode III indicates the correct effect of Y/E but falls below the observed critical radius.

5. In regard to the transition temperature for welded low carbon steel, the effect of plastic constraint induced by double grooved specimens can cause a 40°C rise in fracture transition temperature above that observed by the Charpy specimen. Thus under some conditions the Charpy test may be grossly unconservative.

6. Studies of numerical methods based on a boundary integral method and dislocation modeling of plasticity within elements showed an instability which could be suppressed in creep, but required enough computation with influence coefficients so that it does not appear competitive with finite element methods, except for small plastic zones around cracks in large bodies.

9. Bibliography

Andresen, J. A. 1973 "The Range of Validity of the J Integral for Predicting Fracture in Steel", S.M. Thesis, Dept. of Mech. Eng., M.I.T., Cambridge, MA.

Begley, J. A., Landes, J. D. 1972 "The J Integral as a Failure Criterion" ASTM STP 514, 1-20.

Berg, C. A. 1970 "Plastic Dilatation and Void Interaction" Inelastic Behavior of Solids, M. F. Kanninen, W. F. Adler, R. I. Rosenfield, R. I. Jaffee, eds., McGraw-Hill, New York, 171-210.

Bridgman, P. W. 1952 "Studies in Large Plastic Flow on Fracture" McGraw-Hill, New York.

Cipolla, R. C. 1973 "A Study of the Initiation of Ductile Fracture from Grooves", M.S. Thesis, Dept. of Mech. Eng., M.I.T., Cambridge, MA.

Elliott, D. Stuart, H. 1968 "Fractographic Features Associated with General Yielding in Low Strength Steels", Proc. 3rd Scanning Electron Microscope Symp., Ill., Inst. Tech., Chicago, 305-312.

Hayden, H. W. Floreen, S. 1969 "Observations of Localized Deformation during Ductile Fracture" Acta Met., v.17, 213-224.

Hutchinson, J. W. 1968a "Singular Behavior at the End of a Tensile Crack in a Hardening Material" J. Mech. Phys. Solids, v. 16, 13-31.

Hutchinson, J. W. 1968b "Plastic Stress and Strain Fields at a Crack Tip" J. Mech. Phys. Solids, v. 16, 337-347.

Joyce, J. A. 1968 "Tensile Plastic Deformation at Notch Roots: M.S. Thesis, Dept. of Mech. Eng., M.I.T. Cambridge, MA.

Joyce, J. A. 1974 "On the Mechanisms and Mechanics of Plastic Flow and Fracture" SCD thesis, M.I.T. Dept. of Mech. Eng., Cambridge, MA.

Joyce, J. A., McClintock, F. A., 1976 "Predicting Ductile Fracture Initiation in Large Parts" Strength and Structure of Solid Materials, H. Miyamoto, et al, eds., Noordhoff, Leyden, 157-181.

Levy, N.
Marcal, P.V.
Ostergren, W. J. 1971 "Small Scale Yielding Near a Crack in a Plane Strain: A Finite Element Analysis" Int. J. Fract. Mech., v. 7, 143-156.

Ludwik, P. 1926 Z. Metallkunde, 18, 269.

Marcoli, R. 1975 "Notch Toughness Requirements for Welded Plate, and a Proposed Test", Master's Thesis, Depts. Ocean Eng. and Mech. Eng., M.I.T., Cambridge, MA.

McClintock, F. A. 1968 "A Criterion for Ductile Fracture by the Growth of Holes", J. Appl. Mech. v.35, 363-371.

McClintock, F. A. 1971 "Plasticity Aspects of Fracture", Fracture, v. 3, H. Liebowitz, ed., Acad. Press, New York, 47-225.

McClintock, F. A. 1977a "Mechanics in Alloy Design", Fundamental Aspects of Alloy Design, R. I. Jaffee and B. A. Wilcox, eds., Plenum, New York, 147-172.

McClintock, F. A. 1977b "Plastic Flow around a Crack under Friction and Combined Stress", Fract. 1977, Proc. 4th Intl. Conf. on Fract., Waterloo, Canada, D.M.R. Taplin, ed., Univ. of Waterloo Press, v. 4, 49-64.

Nagpal, V. 1973 "Traction-Displacement Boundary Conditions for Plastic Fracture by Hole Growth", Foundations of Plasticity, A. Sawczuk, ed., Noordhoff, Groningen, 365-385.

Plateau, J.,
Henry, G.,
Crussard, C. 1956 Comptes Rendu, Intl. Cong. Electron Microscopy, Liege, May 1956. Revue Univ. de Mines, 543.

Rice, J. R.
Rosengren, G. F. 1968 "Plane Strain Deformation Near a Crack Tip in a Power-Law Hardening Material" J. Mech. Phys. Solids, v. 16, 1-12.

Rice, J. R.
Tracey, D. M. 1969 "On the Ductile Enlargement of Voids in Triaxial Stress Fields", J. Mech. Phys. Solids, v. 17, 201-217.

Tipper, C. F. 1949 "The Fracture of Metals" Metallurgia, v.39, 133-137.

Rice, J. R.
Johnson, M. A. 1970 "The Role of Large Crack Tip Geometry Changes in Plane Strain Fracture" Inelastic Behavior of Solids, M. F. Kanninen et al, eds., McGraw-Hill, New York, 641-672.

Rice, J. R.
Paris, P. C.
Merkle, J. G. 1972 "Some Further Results of J-Integral Analysis and Estimates", Progress in Flaw Growth and Fracture Toughness Testing, ASTM STP 536, 231-245.

Rice, J. R. 1973 "Elastic-Plastic Fracture Mechanics", Fract. Mech. v. 5, 1019-1022.

Tracey, D. M. 1971 "Strain-Hardening and Interaction Effects on the Growth of Voids in Ductile Fracture" Eng. Fract. Mech., v. 3, 301-315.

Zaverl, F., Jr. 1974 "The Influence of Specimen Dimensions on a J_c Fracture Toughness Test", M.S. Thesis, Univ. of Ill., Theo. and Appl. Mech. Dept., Urbana, Ill.

Appendix: Papers and Degrees

Papers published with the support of the contract:

Joyce, J. A. McClintock, F. A.	1976	"Predicting Ductile Fracture Initiation in Large Parts", Strength and Structure of Solid Materials, H. Miyamoto, T. Kunio, H. Okamura, V. Weiss, M. Williams, S. H. Liu, eds. Noordhoff, Leyden, pp. 157-181.
McClintock, F. A.	1977	"Mechanics in Alloy Design", Fundamental Aspects of Structural Alloy Design, R. I. Jaffee, ed., Plenum Press, New York, pp. 147-172.

Degrees earned by students supported under the contract:

J. A. Andresen, M. S. in Mechanical Engineering, August, 1973

J. A. Joyce, Sc.D. in Mechanical Engineering, May, 1974.